Laser and Particle Beams (2017), *35*, 326–336.
© Cambridge University Press, 2017 0263-0346/17
doi:10.1017/S0263034617000180

Two-frequency undulator usage in compact self-amplified spontaneous emission free electron laser in Roentgen range

K. ZHUKOVSKY AND I. POTAPOV

Faculty of Physics, M.V. Lomonosov Moscow State University, Leninskie Gory, Moscow, 119991, Russia

(RECEIVED 14 January 2017; ACCEPTED 20 February 2017)

Abstract

The generation of harmonics in two-frequency undulator in a self-amplified spontaneous emission free electron laser (SASE FEL) is studied in order to produce Roentgen radiation in a relatively compact sized installation. The dynamics of SASE FEL is analyzed with the help of the phenomenological model to obtain the maximum of the X-ray high-harmonic power. The model accounts for the properties of the undulator magnetic field and of the electron beam and includes the major sources of losses, such as the electron energy spread, etc. It is compared and calibrated with the existing data on a FEL experiment. The advantages of the two-frequency undulator for Roentgen SASE FEL are demonstrated and the possibility to generate powerful mild Roentgen radiation at already ~25 m length is shown. The evolution of the bunching coefficients for high harmonics is studied together with the evolution of the FEL-induced energy spread. The linear and non-linear regimes are explored for common and for two-frequency undulators The usage of the two-frequency undulator for cascade SASE FEL with high X-ray harmonic power and high-harmonic bunching coefficients with low-induced energy spread is proposed.

Keywords: Undulator radiation; Harmonic radiation; Free electron laser (FEL); Two-frequency undulator

1. INTRODUCTION

Synchrotron radiation (SR) and undulator radiation (UR) were discovered more than 50 years ago; their importance for researchers now comes due to their numerous applications. The undulator working principle consists in that relativistic charges emit radiation in narrow angle along the undulator axis, while moving with relativistic drift along the undulator with weak transversal oscillations; it selects few radiated harmonics. This principle was proposed by Ginzburg (1947), and then the undulator was built by Motz *et al*. (1953). The UR theory was consequently developed [see, e.g., Artcimovich & Pomeranchuk (1945); Alferov *et al.* (1973); Ternov *et al.* (1985); Alferov *et al.* (1989); Bordovitsyn (1999)]. Researchers repeatedly returned to the UR studies due to reasons, which varied with time passing. In the last decade, the interest to the UR was in big part due to free electron lasers (FELs) development, including FEL with single pass of the radiation. These sources produce extremely intense radiation and thus they are particularly interesting from practical view point, especially for studying the interaction of this radiation with matter Ziaja *et al*. (2007), for plasma production and properties studies, as seen in the works of Lee *et al*. (2002), Zastrau *et al*. (2012), Bartnik *et al*. (2013) and of other researchers. Contrary to common radiation sources FEL are capable of generating megawatt and even gigawatt power in short interval of time ~femtosec. Recent efforts are aimed on construction of sources, capable of radiating significant power in Roentgen range (see Bessonov *et al*. 2008; Huang & Tallents, 2009; Kumar *et al.*, 2012; Artyukov *et al*., 2016), which allows studying physical processes on nanometric scale. Moreover, recent papers report on angstrom-wavelength FELs (see, for example, Emma *et al*. (2010)). At such high frequencies the mirror FEL design is difficult to implement due to lack of materials capable of reflecting radiation in Roentgen range. Thus, self-amplified spontaneous emission (SASE) FELs are best candidates, despite they have their disadvantages too. Such SASE FEL requires high-energy electrons and it takes hundreds of meters and dozens of undulator segments to generate the fundamental harmonic in Roentgen range as demonstrated, for example, by Zhirong and Kwang-Je (2007), McNeil and Thompson (2010) etc. Thus, proper installations, for example, X-FEL, LCLS, etc., become increasingly expensive and laborious to construct and exploit.

Address correspondence and reprint requests to: K. Zhukovsky, Faculty of Physics, M.V. Lomonosov Moscow State University, Leninskie Gory, Moscow, 119991, Russia. E-mail: zhukovsk@physics.msu.ru

https://doi.org/10.1017/S0263034617000180 Published online by Cambridge University Press

Modern undulator constructions allow for effective harmonic regulation by secondary periodic fields, additional to the main periodic magnetic field of a common planar or helical undulator. It allows suppressing or enhancing certain UR harmonics selectively [see, e.g., Dattoli *et al.* (2006*a*); Bessonov (2007); Mishra *et al.* (2009); Tripathi & Mishra (2011); Zhukovsky (2012, 2015*a*, *b*)]. To make full advantage of these exotic undulator schemes the quality of the devices and of the beams should be high. The most serious deterioration of the UR lines, perhaps, comes due to the electron energy spread, although the contribution of other factors, such as non-periodic magnetic components, beam divergence etc. also should not be neglected. Their analytical account in the case of the spontaneous UR was recently described, for example, by Zhukovsky (2016*a*). It was also concluded by Vagin *et al.* (2011) that in modern undulator devices the quality of the UR lines is in fact determined almost exclusively by the electron beam quality. Low-energy electron beams usually have high quality and they are closer to the ideal monoergetic non-divergent beam. Moreover, they can be sourced at much lower cost and they are frequently used for UV FELs [see, e.g., Giannessi *et al.* (2011); Dattoli *et al.* (2014); Mirian *et al.* (2014)].

The goal of the present study is to demonstrate that it is possible to generate Roentgen frequencies at least in mild-Roentgen range in relatively compact devices of the scale of few dozens of meters, which are much smaller than the commonly used giant X-FEL installations. To this end we will use a simple phenomenological model of SASE FEL, accounting for both: linear and nonlinear harmonic generation, as well as for major losses, such as those due to the electron energy spread and other. With its help we will analyze the dynamics of SASE FEL power and of the bunching coefficients along SASE FEL and identify the requirements for the undulator and for the electron beam to generate intense Roentgen radiation ~0.1–100 MW.

2. PHENOMENOLOGICAL MODEL OF SASE FEL

The analysis of spontaneous UR with account for major sources of spectral line broadening is best done with the help of the generalized special functions of Bessel and Airy type, which describe respectively the UR spectrum and the shape of the UR lines, as done, for example, by Dattoli *et al.* (2008, 2009), Mikhailin *et al.* (2014), Zhukovsky (2014*a*, *b*, *c*), and give exact account for the finite size of the beam, its divergence, energy spread, etc. (see, e.g., Quattromini *et al.* (2012); Zhukovsky (2015*c*, 2016*b*)). As regards SASE FEL dynamics, basic equations for its analytical model were developed by Dattoli *et al.* (2004, 2005*a*, *b*), and applied also in the common work with Dattoli *et al.* (2006*a*). However, the above-cited works contain some inconsistencies and misprints, which frequently yield unphysical results, if the formulae are applied literally. In particular, it regards nonlinear regime for high harmonics, especially in segmented devices, and account for the losses. We remind that the wavelength of the radiated nth UR harmonic of a common planar undulator reads as follows:

$$\lambda_n = \frac{\lambda_0}{n}, \quad \lambda_0 = \frac{\lambda_u}{2\gamma^2}\left(1 + \frac{k^2}{2}\right), \tag{1}$$

where γ is the relativistic parameter, λ_u is the undulator period, and k is the undulator parameter

$$k = eH_0\lambda_u/2\pi mc^2, \quad k^2 = 2\gamma^2\beta_\perp^2, \tag{2}$$

$\beta_\perp$ is the electron velocity component, normal to the undulator axis, H_0 is the strength of the undulator magnetic field, e and m are the electron charge and mass, and c is the speed of light. Consider the planar two-frequency undulator of N periods with the following magnetic field:

$$\begin{gathered}\vec{H} = H_0(\rho, \kappa + \sin(k_\lambda z) + d\sin(hk_\lambda z), 0), \\ h \in Z, \quad \rho, \kappa = \text{const}.\end{gathered} \tag{3}$$

The non-periodic magnetic components $H_x^{\text{const}} = \rho H_0$ and $H_y^{\text{const}} = \kappa H_0$ yield the effective bending angle $\theta_H = (2/\sqrt{3})(k/\gamma)\pi N\kappa_1$, which depends on the total strength of the constant magnetic component via the parameter $\kappa_1 = \sqrt{\kappa^2 + \rho^2}$. Its influence is similar to that of the off-axis deviation in the angle θ_H. The UR intensity with account for the divergence reads (see Zhukovsky, 2016*b*) as follows:

$$\begin{aligned}\left.\frac{d^2I}{d\omega d\Omega}\right|_{(H_d/H_0)^2 \ll 1/(4\pi N)^2} &\cong \frac{e^2N^2\gamma^2}{c}\frac{k^2}{(1 + k_{\text{eff}}^2/2)^2} \\ &\times \sum_{n=1}^{\infty} n^2\left[S(\alpha, \beta, \eta)\left(T_{n-1} + T_{n+1} + \frac{d}{h}(T_{n+h} + T_{n-h})\right)\right]^2,\end{aligned} \tag{4}$$

where $k_{\text{eff}}^2 = k^2 + k_2^2$, $k_2 = k|d/h|$, and it depends on the generalized Airy-type function $S(\alpha, \beta, \eta) \equiv \int_0^1 d\tau e^{i(\alpha\tau + \eta\tau^2 + \beta\tau^3)}$, as demonstrated, for example, in the recent work by Zhukovsky (2015*c*), and on the generalized Bessel functions

$$\begin{aligned}T_n = \int_0^{2\pi}\frac{d\varphi}{2\pi}\cos n &\left[\varphi + \frac{k^2\sin(2\varphi)}{4(1 + k_{\text{eff}}^2/2)} - \frac{dk^2\sin((h-1)\varphi)}{h(h-1)(1 + k_{\text{eff}}^2/2)} - \right. \\ &\left. \frac{dk^2\sin((h+1)\varphi)}{h(h+1)(1 + k_{\text{eff}}^2/2)} - \frac{d^2k^2\sin(2h\varphi)}{4h^3(1 + k_{\text{eff}}^2/2)}\right].\end{aligned} \tag{5}$$

The non-periodic magnetic components $H_x^{\text{const}} = \rho H_0$, $H_y^{\text{const}} = \kappa H_0$ are accounted for by the parameter $\beta = ((2\pi nN + \nu_n)(\gamma\theta_H)^2/1 + (k^2/2)(1 + (d/h)^2) + (\gamma\theta_H)^2)$, $\nu_n = 2\pi Nn((\omega/\omega_n) - 1)$ is the detuning parameter, the off-axis angles $\Theta_{x,y}$ interplay with κ_1 in the parameter $\eta = ((2\pi N)^2 nk\gamma/1 + k^2/2 + (\gamma\psi)^2)(\kappa\Theta_x - \rho\Theta_y)$, where

https://doi.org/10.1017/S0263034617000180 Published online by Cambridge University Press

$\theta_H = (2/\sqrt{3})(k/\gamma)\pi N\kappa_1$, and the sum of their squares constitutes the angle $\psi = \sqrt{\Theta_x^2 + \Theta_y^2}$ in $\alpha = \nu_n + (2\pi nN(\gamma\psi)^2/1 + (k^2/2) + (\gamma\psi)^2)$; they are the parameters of the generalized Airy function $S(\alpha, \beta, \eta)$. The resonance frequencies read

$$\omega_n = n\omega_R = \frac{2n\omega_0\gamma^2}{1 + (k_{eff}^2/2) + (\gamma\psi)^2 + (\gamma\theta_H)^2 - \gamma^2\theta_H\psi\sqrt{3}((\rho\sin\phi - \kappa\cos\phi)/\kappa_1)}, \quad (6)$$

where $\omega_0 = 2\pi c/\lambda_u(1 - (1/2\gamma^2)(1 + (k^2/2)))$, φ is the polar angle. In the case of the common planar undulator with purely periodic magnetic field, the generalized Airy function reduces $S^2 \to sinc^2(\nu_n/2)$ and the only non-vanishing polarization component depends on the common Bessel function: $T_{n,x} \to (J_{n+1/2}(-\xi/8) + J_{n-1/2}(-\xi/8))$, $\xi = -k^2/4/(1 + (k^2/2)(1 + (d/h)^2))$. The conditions when the usage of the above common formulae are possible and the necessity of compensation of non-periodic magnetic components was discussed, for example, in Mikhailin *et al.* (2014), Zhukovsky (2014*a*, *b*, *c*). For a common planar undulator it is enough to assume $d = 0$ in (4)–(5) and in all following results.

It should be kept in mind that the electrons in the beam have different from each other energies, velocities, and positions respectively to the axis, which results in deviation off the axis in the angles $\Theta_{x,y}$. The description of the losses due to the above mentioned factors and their effect on the UR lines shape and intensity can be done with the help of the convolution, as proposed, for example, by Dattoli (1993):

$$I = \iiint d\varepsilon d\Theta_{x,y}\,(|S(\nu_n + 4\pi N\varepsilon n, \beta, \eta)|)^2 \exp[-\varepsilon/2\sigma_\varepsilon^2]/(\Theta_{x,y\max}\sigma_e\sqrt{2\pi}), \quad (7)$$

where σ_e is the energy spread, ν_n is the detuning parameter, $\Theta_{x,y\max} = \varepsilon_{x,y}/\sigma_{x,y}$ are the beam divergences, $\varepsilon_{x,y}$ are the beam emittances, $\sigma_{x,y}$ are the cross-sections, related to the emittances as follows:

$$\sigma_{x,y} = \sqrt{\varepsilon_{x,y}\beta_{x,y}}, \quad \Theta_{x,y} = \sqrt{\varepsilon_{x,y}/\beta_{x,y}}, \quad \sigma_{x,y}\Theta_{x,y} = \varepsilon_{x,y}, \quad (8)$$

where $\beta_{x,y}$ are the Twiss coefficients, standing for local focal lengths of the magnetic system of the undulator, chosen in an optimal way for beam matching [see Dattoli (1993) for details].

The evolution of the radiated power and of the bunching coefficients along SASE FEL depends on the fundamental Pierce parameter:

$$\rho_n = \frac{1}{2\gamma}\left(\frac{J}{2\pi i}(\lambda_u k_{eff} f_n)^2\right)^{1/3}, \quad (9)$$

where $f_n = (-1)^{n-1/2}\ (T_{n-1} + T_{n+1} + (T_{n+h} + T_{n-h})d/h)$, J is the electron current density (A/m^2), $i = 1.704509 \times 10^4$ is the Alfven current (A), n is the harmonic number. It is well known that for a stable amplification in SASE FEL the quality of the beam must be good enough and the broadening coefficients for broadening factors, such as the energy spread, divergence, etc. must be below unity, yielding the respective conditions $\varepsilon_{x,y} \le \lambda_0/4\pi$ and $\sigma_\varepsilon \le \rho/2$. The Pierce parameter ρ_n renormalized as $\tilde{\rho}_n = n^{1/3}\rho_n$ defines for the harmonic with the number n its characteristic gain length $L_{n,g} = \lambda_u/(4\pi\sqrt{3}\tilde{\rho}_n)$ and its maximal power $P_{n,F} = P_F/\sqrt{n}(f_n/nf_1)^2$, where $P_F \cong \sqrt{2}\rho_1 P_e$ is the power of the fundamental harmonic and P_e is the electron beam power. The SASE FEL harmonic power grows from the seeded power $P_{0,n}$ and reaches the saturation at the length $Z_s \cong 1.066L_{1,g}\ln(9P_F/P_0)$, following the exponential law (see Dattoli *et al.*, 2006*a*):

$$P_{L,n}(z) \cong P_{0,n}\frac{A(n,z)\exp(0.223z/Z_s)}{1 + (A(n,z) - 1)P_0/P_F}, \quad (10)$$

where

$$A(n,z) \cong \frac{1}{9}\left(3 + 2\cosh\left(\frac{z}{L_{n,g}}\right) + 4\cos\left(\frac{\sqrt{3}z}{2L_{n,g}}\right)\cosh\left(\frac{z}{2L_{n,g}}\right)\right). \quad (11)$$

For a prebunched beam the formula modifies accordingly to describe immediate growth without lethargy domain from the power, provided by the bunching. The radiation frequencies of a planar undulator (1) are at even harmonics with $n = 1, 3, 5,\ldots$. The fundamental harmonic gives the most FEL power, the FEL subharmonics are weaker and their intensities depend as on the respective Bessel function values as on the radiation of the fundamental harmonic, being the product of the whole complex of phenomena of the interaction of the radiation emitted at resonant frequencies $\omega_{n=1,3,5,\ldots}$ with the electron bunch. The sub harmonics power growth is well known to occur first following the main FEL tone at a lower power and rate; then the nonlinear regime kicks in, and the nth harmonic grows faster, following the nth power of the fundamental: $Q_n(z) \propto e^{nz/L_g = L_{1,g}}$. This process ends with the saturation regime on the length $Z_{s,n}$, close to that of the fundamental Z_s. The radiation power of the subharmonics of the fundamental, $P_n = P_{L,n} + Q_n$, thus consists of the so-called linear component (10), (11) and of the non-linear component as described by

https://doi.org/10.1017/S0263034617000180 Published online by Cambridge University Press

Dattoli *et al.* (2005*b*, *2006a*):

$$Q_n(z) \cong P_{n,0}\frac{\exp(nz/L_g)}{1+(\exp(nz/L_g)-1)P_{n,0}/P_{n,F}}. \quad (12)$$

The above nonlinear component mostly grows at the end of the undulator as the nth power of the fundamental harmonic power; it begins with the equivalent seeding power $P_{n,0} = d_n b_n^2 P_{n,F}$ and reaches its saturated power $P_{n,F} \cong (1/\sqrt{n})(f_n/nf_1)^2 P_F$, where b_n are the bunching coefficients and $d_3 \approx 8$, $d_5 \approx 116$ are the engineering constants for $n = 3,5$.

3. ACCOUNT FOR THE ELECTRON BEAM QUALITY

Exact account for the losses in the undulator is possible with the help of the convolution (7). Take note, that high harmonics are much more sensitive to the beam quality and are much more subjected to losses due to the dependence on n in (7): $S(\nu_n + 4\pi N\varepsilon n)$. This influence was thoroughly explored in the case of the spontaneous UR in the array of works by Zhukovsky (2015*a*, *b*, *c*, 2016*a*, *b*). However, due to rather complicated mathematical forms of integrals of generalized special functions, involved in (7), we do not think it is worth including this rigorous formalism in the simple phenomenological model of SASE FEL. We will limit ourselves to much simpler formalism of broadening or otherwise loss coefficients μ_i, describing the effective losses due to the factor i, in analogy with that done for the spontaneous UR [see, e.g., Zhukovsky (2014*a*, *c*)]; this approach seems more adequate the level of the complexity and the precision of our phenomenological model. Perhaps, the major source of losses still remains the electron energy spread, which can seriously deteriorate and even ruin the FEL operation. In particular, the energy spread increases the gain length L_g and reduces the FEL power P_F. To keep this negative effect low, FEL should be fed with highly monoenergetic beam, where $\sigma_\varepsilon \le \rho/2$. Importantly, following the convolution (7), we now include in the nth harmonic energy spread coefficient the dependence on the harmonic number n:

$$\mu_{\varepsilon,n} = 2n\sigma_\varepsilon/(n^{1/3}\rho_n). \quad (13)$$

This increases the gain length for the harmonics dependently on their number:

$$L_{n,g} \to L_{n,g}\Phi(\mu_{\varepsilon,n}) \quad (14)$$

and reduces their saturated power:

$$P_{n,F} \to P_{n,F}\eta(\mu_{e,n}) \quad (15)$$

with the help of the *ad hoc* chosen functions

$$\Phi(\mu_{\varepsilon,n}) = (\zeta + 0.18\mu_{\varepsilon,n}^2)\exp(0.034\mu_{\varepsilon,n}^2), \quad \zeta = 1, \quad (16)$$

and

$$\eta(\mu_{\varepsilon,n}) = \left(\exp(-(\Phi(\mu_{\varepsilon,n}) - v)\Phi(\mu_{\varepsilon,n})) + \sqrt{2}\frac{\Phi(\mu_{\varepsilon,n}) - v}{v(\Phi(\mu_{\varepsilon,n}))^3}\right)/w,$$
$$v = 0.9, \quad w = 1.062. \quad (17)$$

The eminent divergence of the beam is effectively accounted for by the coefficient ζ in (16), which depends on the proper coefficients $\mu_{x,y}$, which in turn can increase the value of ζ up to $\approx$1.2 in the case of significant divergence, thus extending the gain and the saturation lengths. Proper relation for $\zeta(\mu_{x,y})$ can be derived from expressions found in FEL handbooks, such as Dattoli *et al.* (2007), and they do not qualitatively change the behavior of (16), but they make it more cumbersome; we omit them for brevity. For a well-matched good quality beams this contribution is minor and we can consider $\zeta = 1-1.1$. Other parameters in (16) were chosen based on the comparison with the experimental data and with the results of numerical simulations of FEL dynamics in C++, available in Dattoli *et al.* (2004). In particular, for the power correction we have chosen $v = 0.9$, $w = 1.062$ [see Fig. 1. Function $\eta(\mu_{\varepsilon,n})$ – blue line for $v = 0.9$, $w = 1.062$ [see (17)]. Previously used function – red line for $v = w = 1$].

This eliminates unphysical behavior of the previously used by Dattoli *et al.* (2004) function with $v = w = 1$, which resulted in growth of the saturated power when μ_ε is close to, but not equal zero, and for respective energy spread $\sigma_\varepsilon \neq 0$. Moreover, our new corrections (13)–(17) now differentiate the harmonics and have stronger effect on high FEL harmonics as it generally speaking should be according to (7).

The diffraction for the finite sized electron beam can be accounted for on the base of the beam divergence, emittance, the undulator period λ_u, and the wavelength λ_n, by modifying the Pierce parameter for the proper harmonic n as proposed,

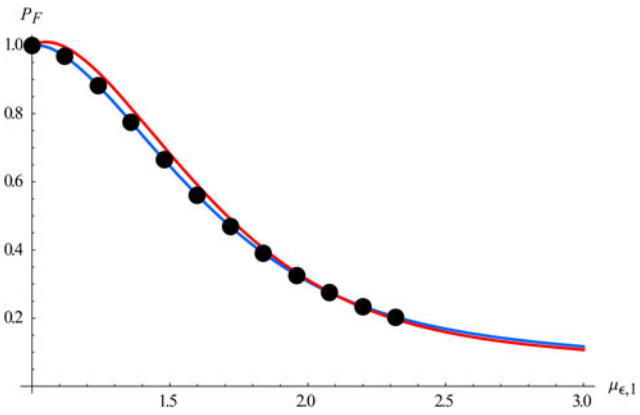


Fig. 1. Function $\eta(\mu_{\varepsilon,n})$ – blue line for $v = 0.9$, $w = 1.062$ (see. (17)). Previously used function – red line for $v = w = 1$.

https://doi.org/10.1017/S0263034617000180 Published online by Cambridge University Press

for example, in the following work of Dattoli *et al.* (2005*b*):

$$\rho_n \to \rho_{\mathrm{D},n} = \frac{\rho_n}{(1+\mu_{\mathrm{D},n})^{1/3}}, \quad \mu_{\mathrm{D},n} = \frac{\lambda_\mathrm{u}\lambda_n}{(4\pi)^2\rho_n\sigma}, \tag{18}$$

where $\sigma = P_\mathrm{e}/\pi E_\mathrm{e}\gamma j$ is the beam cross section, related to the beam power P_e and current density j, where $E_\mathrm{e} = 0.5109989\times10^6$ is the electron energy (eV), γ is the relativistic factor, $j = I_0/(\pi\sigma)$ is the current density in a Gauss beam ($\mathrm{A/m^2}$), I_0 is the beam current (A). More elaborated account can be done separately for x and y-coordinates, explicitly involving Twiss parameters as described by Dattoli *et al.* (2004)) and making more complicated the dependence (18), but the essence of the latter relation remains unchanged. In the framework of our phenomenological model this seems just an excessive complication and formula (18) appears sufficient. In what follows we will demonstrate it by comparison with an experiment and with numerical simulations. So, corrected bunching coefficient now becomes:

$$b_n = \left(P_0/9P_\mathrm{e}\rho_{\mathrm{D},1}\right)^{n/2}. \tag{19}$$

Not going deep into the details, we mention that the whole complex of the processes in SASE FEL essentially includes the interaction of the intense electromagnetic fields of the radiated frequencies with the electrons of the beam. At a certain point the radiated FEL power reaches its saturation; this process is accompanied by significant FEL induced energy spread of the electrons in the beam, increasing along the FEL length and usually exceeding by far the initial energy spread of the electron source. The FEL induced energy spread is relevant to the wave-electron beam interaction close to the saturation regime, differently from the initial energy spread, which can be rather low just out of a LINAC. The full energy spread is described by the well-known formula

$$\sigma_\varepsilon^2(z) = \sigma_{\varepsilon,0}^2 + \sigma_{\mathrm{FEL}}^2(z), \tag{20}$$

where $\sigma_{\varepsilon,0}$ is the initial energy spread in the beam and [see, e.g., Dattoli *et al.* (2007)] the FEL induced energy spread reads as follows

$$\sigma_{\mathrm{FEL}}^2(z) = \frac{3}{2}\sqrt{\frac{\rho_{\mathrm{D},1}P_0A(1,z)}{P_\mathrm{e}(1+1.24P_0(A(1,z)-1)/P_{1,\mathrm{F}}\eta(\mu_{\varepsilon,1})}}\Bigg|_{\rho\to\rho_{\mathrm{D},1}}, \tag{21}$$

where $\rho \to \rho_{\mathrm{D},1}$ is intended everywhere in A, $P_{1,\mathrm{F}}$, η, etc.

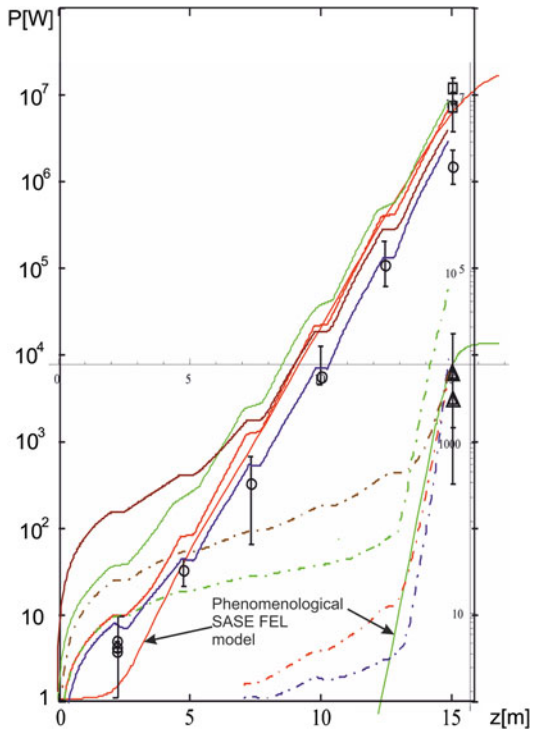


Fig. 2. Simulation of FEL dynamics in phenomenological SASE FEL model: continuous lines, marked by arrows, $n = 1$ – red line, $n = 3$ – green line; numerical simulations results (as reported in Giannessi *et al.* (2011)): $n = 1$ – continuous lines, $n = 3$ – dashed lines; experimental data: $n = 1$ – circles, $n = 3$ – triangles.

4. VALIDATION OF THE PHENOMENOLOGICAL FEL MODEL

Earlier it was shown that main equations, used in the phenomenological model, agree fairly well with some numerical simulations Dattoli (1993), Dattoli *et al.* (2005*a*, *b*, 2006*b*). However, no direct comparison with an experiment has been done. With the improvements and verifications introduced in the present work, in particular those, regarding the high-harmonic power and the account for the losses, we will now validate our phenomenological model by comparing it with the SASE FEL experiment, described by Giannessi *et al.* (2011). The comparison is demonstrated in Figure 2. It comes without saying that we chose the parameters for the simulation exactly matching those in the experiment; most important of them are reported below together with the results of the simulation:

$k = 2.133$, $h = 3$, $d = 0$, $\lambda_\mathrm{u} = 0.028$,
$N_\mathrm{s} = \mathrm{IntegerPart}[L_\mathrm{s}/\lambda_\mathrm{u}] = 599$, $L_\mathrm{s} = 16.5$ m, $L_\mathrm{gain} = 0.8265$ m,
$\gamma = 301.37$, $P_\mathrm{E} = 8.624$ GW, $J = 1.9\times10^8$ $\mathrm{A/m^2}$,
$\Sigma_\mathrm{ebeam} = 9.38\times10^{-8}$ $\mathrm{m^2}$, $I_0 = 56$ A, $\sigma_\varepsilon = 0.0009$,
$\lambda_1 = 504.799$ nm, $\lambda_3 = 168.266$ nm, $\lambda_5 = 100.96$ nm,
$\rho_n = \{0.0020973,\ 0.00116213,\ 0.000834944\}$,
$\rho_n^\mathrm{D} = \{0.00185089,\ 0.0010721,\ 0.000779581\}$,
$\Phi_n = \{1.18916,\ 4.47213,\ 39.1083\}$,
$\eta_n = \{0.922068,\ 0.0590925,\ 0.000945145\}$,
$P_\mathrm{F} = 20.8146\times10^6$ W,
$P_{n,\mathrm{F}} = \{20.8146\times10^6,\ 14558.4,\ 24.0808\}$ W,
$b_n = \{0.0000834322,\ 5.80767\times10^{-13},\ 4.04268\times10^{-21}\}$.

From (1) we obtain the radiation of the fundamental harmonic at the wavelength $\lambda_0 \approx 500$ nm and the saturation

https://doi.org/10.1017/S0263034617000180 Published online by Cambridge University Press

wavelength $L_s = 16.5$ m in agreement with that stated by Giannessi *et al.* (2011) and put by the authors as "at 15 m FEL was close to the saturation".

It follows from Figure 2 that the phenomenological SASE FEL model not only qualitatively describes the experiment, but it also correctly reproduces the power growth, the saturated power and saturated length values and it also gives correct value for the third harmonic evolution and its saturated power. Moreover, as seen in Figure 2 our account for the losses, which is now harmonic number dependent, gives much better agreement with the experiment that most of the numerical simulations, even those in three-dimensional (3D) in C++, all shown in Figure 2 for comparison. Indeed, the dynamics of the third harmonic is such, that its growth over $P_0 = 1$ W seed power of the fundamental harmonic occurs after 12 m, and it is due to the nonlinear power growth mentioned above. Most of the numerical simulations predicted much earlier growth seemingly in the linear regime (see dash-dotted lines at lengths <12 m), which, however, was not detected. It should be mentioned, that if we did not introduce harmonic dependent loss coefficient (13) and consequent correction (16), (17), sticking to the commonly used formulae, given in handbooks (example.g., Dattoli *et al.* (2007)), and then the predicted values for the third harmonic in particular would be much higher than those measured. We omit proper figure since it disagrees with the experiment.

So, our phenomenological model with harmonic dependent loss coefficient (13) and consequent corrections (16), (17) predicts correct saturated value at 15 m and rapid power growth in nonlinear regime just before 15 m, which totally agrees with the experiment. Thus, we have got good account for the beam properties. Previously used by Dattoli *et al.* (2005*b*, 2007), formulae give too high values for the third harmonic power, too early growth in linear regime as results also from all numerical simulations reported in Figure 2 (see dash-dotted lines at lengths <12 m). We do not speculate on possible reasons for that, but underline that the simple phenomenological model is fully capable of giving correct predictions, which are sometimes even better than complicated numerical 3D simulations. As for the disagreement with the measurements at the first 2 m interval, we implied in the model the seed and initial lethargy regime, while in the experiment, possibly, fairly big amount of the initial shot noise was present, which led to this disagreement. Proper account for it will be introduced elsewhere.

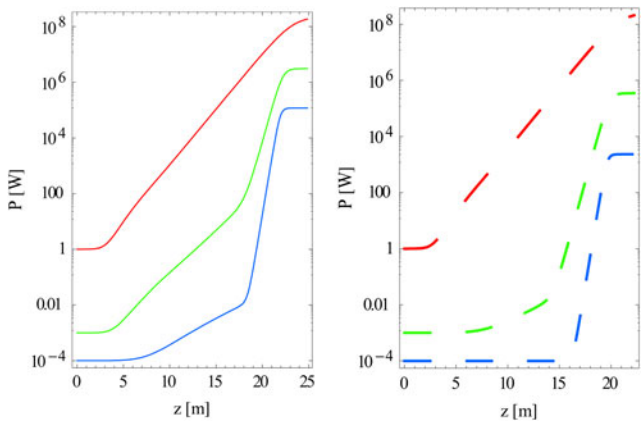


Fig. 3. Evolution of the SASE FEL harmonic power with the two-frequency planar undulator with c $k = 2.133$, $h = 3$, $d = -0.5$ (left) and with the common planar undulator with $d = 0$ (right). The harmonic frequencies for the two-frequency undulator are $\lambda_1 = 20.5816$ nm, $\lambda_3 = 6.86053$ nm, $\lambda_5 = 4.11632$ nm (left) and for the common undulator: $\lambda_1 = 20.192$ nm, $\lambda_3 = 6.73066$ nm, $\lambda_5 = 4.03839$ nm (right). The values of the parameters of the undulator and of the beam: $\lambda_u = 0.028$ m, $\gamma = 1506.85$, $P_E = 103.95$ GW, $J = 9.96573 \times 10^9$ A/m^2, $I_0 = 135$ A, $\Sigma_{ebeam} = 4.31362 \times 10^{-9}$ m^2, $\sigma_\varepsilon = 0.0005$. The harmonics are denoted as follows: $n = 1$ – red line, $n = 3$ – green line, $n = 5$ – blue line.

It should be underlined that FEL dynamics is a product of the whole complex of the processes of interaction of the radiation with the electron beam, which includes the electron beam energy modulation, bunching, incoherent, and coherent radiation, bunching on the sub harmonic wavelengths and their radiation and eventually the saturation. Clearly, complete and precise description of these processes cannot be done in the framework of a simple phenomenological model fitted with very few parameters. However, the comparison with the experiment reveals surprisingly good agreement, which means that the model catches well the main features of the FEL dynamics even for high harmonics and surprisingly excels even when compared with very complex numerical simulations requiring significant computation facilities.

5. SASE FEL WITH TWO-FREQUENCY UNDULATOR FOR ROENTGEN BAND

We can now apply the validated phenomenological SASE FEL model for the simulation of the performance of SASE FEL in Roentgen range. It is well known that Roentgen laser requires high-energy electron sources and significant size of the installation. This latter increases the building and exploitation costs; moreover, on a long distance the electron bunch and the photon radiation change their positions with respect to each other, the beam divergence cannot be neglected so that the beam should be regularly refocused; the electron energy spread also grows. Thus, it would be advantageous to obtain high-frequency radiation in an installation of a moderate scale, reducing all the above mentioned drawbacks of the present large devices. Keeping this in mind, we will model the performance of a FEL with the two-frequency undulator in order to obtain soft Roentgen radiation. We can even choose the undulator with the same parameters as used for 500 nm FEL experiments Giannessi *et al.* (2011), but with the additional second periodic field [see (3)], so that its parameters are as follows: $k = 2.133$, $h = 3$, $d = -0.5$, $\lambda_u = 0.028$ m and high-quality electron beam of the energy and the energy spread respectively $E = 0.77$ GeV, $\sigma_\epsilon = 0.0005$; other parameters are as follows: $\gamma = 1506.85$, $P_E = 103.95$ GW, $J = 9.96573 \times 10^9$ A/m^2, $\Sigma_{ebeam} = 4.31362 \times 10^{-9}$ m^2, $I_0 = 135$ A. With this input

https://doi.org/10.1017/S0263034617000180 Published online by Cambridge University Press

we evidently obtain (see (1)) the harmonics at the wavelengths $\lambda_1 = 20.5816$ nm, $\lambda_3 = 6.86053$ nm, $\lambda_5 = 4.11632$ nm, the latter being in the near-Roentgen range. The gain length, the saturation length and the total number of the undulator periods in all sections then read respectively $L_{\text{gain}} = 1.11096$ m, $L_s = 25.1423$ m, $N_s = 898$.

SASE FEL power dynamics simulation with the above given parameters for a common and for two-frequency planar undulator in the framework of our phenomenological model are presented in Figure 3. Continuous lines stand for the two-frequency undulator (left plot): $n = 1$ – red line, $n = 3$ – green line, $n = 5$ – blue line. For comparison we give the simulation of the performance for the common planar undulator, that is with $d = 0$ and with the same value of the undulator parameter $k = 2.133$ [см. (3)]; the electron beam also remains unchanged in this case. As seen in Figure 3 the significant power growth occurs over the 1 W seed power for the fundamental harmonic: 10^8 times, and for the subharmonics: 3×10^6 times for $n = 3$ and 10^5 for $n = 5$ at the wavelength of $\lambda_5 = 4.11632$ nm, which is in the near Roentgen range. Note from the comparison of the plots in Figure 3 (left plot is for the two-frequency undulator and right plot is for the common undulator) that the high-harmonic power starts growing much earlier for the two-frequency undulator and its growth occurs much stronger and faster.

Moreover, the nonlinear contribution is less significant for the two-frequency undulator, big part of the harmonic power growth is due to the linear contribution at the beginning and in the middle of the undulator. We remind that this growth, being far from the saturation length is not accompanied by significant induced energy spread. In the common undulator, on the contrary, the high-harmonics grow mostly due to the nonlinear contribution, which is seen in Figure 3 as the rapid power increase at the end of the undulator close to the saturation length. Very important is the fact that the saturated power for the third harmonic in the two-frequency undulator is almost one order of magnitude higher than that for a common undulator and for the 5th harmonic it is almost two (!) orders of magnitude higher for the two-frequency undulator. This is a strong advantage of the two-frequency undulator FEL since it allows the users to get intense Roentgen radiation $\approx$100 kW on $\approx$4 nm after $\approx$22 m length from a relatively low-energy $E \approx 0.75$ GeV beam with low seed power and frequency.

For comparison we simulate the fundamental harmonic generation at the wavelength $\approx$4 nm in FEL with the undulator, having the same parameters as considered before, that is with $k = 2.133$, $\lambda_u = 0.028$ m in Figure 4. Note, that the total length in this case equals $L_s = 67.2624$ m, which implies the total of $N = 2402$ periods (!), while the gain length becomes as long as $L_{\text{gain}} = 3.0431$ m, and the electron beam should have the gamma factor $\gamma = 3315.07$, the power $P_E = 207.9$ GW, the current density $J = 9.96573 \times 10^9$ A/m^2, the beam section is $\Sigma_{\text{ebeam}} = 3.92147 \times 10^{-9}$ m^2, the current $I_0 = 122.7$ A; for the energy spread $\sigma_e = 0.0005$ the fundamental frequency with the wavelength $\lambda_1 = 4.17189$ nm has maximum power $P_{1,F} = 1.11979 \times 10^8$ W.

Note also that the fifth harmonic is practically absent (see Fig. 4), the third harmonic at $\lambda_3 = 1.39063$ nm appears late; it is totally induced by the fundamental one and it is relatively weak at saturation level $P_{3,F} = 10$ kW after 60 m. The saturation of the fundamental harmonic, however, comes after 67 m at high power $\approx$100 MW. Thus, in order to generate the 4 nm Roentgen wavelength by the fundamental harmonic, the FEL installation of roughly 100 m is needed. It is technically cumbersome and complicated problem, not to mention the costs of the building and the operation. Evidently, effective high-harmonic generation, in particular in linear regime, efficiently executed by the two-frequency undulator, reduces dramatically the costs and the total scale of the FEL at the expense of lower saturated power. However, this latter shortcoming can be overcome, if advanced cascade FEL

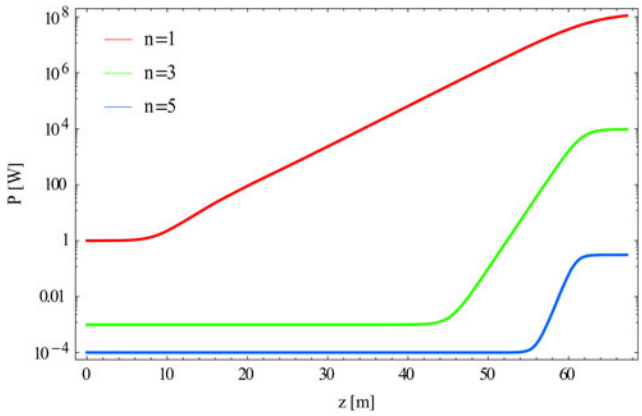


Fig. 4. Evolution of first three odd harmonics along the SASE FEL length (in meters) for the SASE FEL with $k = 2.133$, $\lambda_u = 0.028$, $L_s = 67.2624$ m, $N = 2402$, $L_{\text{gain}} = 3.0431$ m, $\gamma = 3315.07$, $P_E = 207.9$ GW, $J = 9.96573 \times 10^9$ A/m^2, $\Sigma_{\text{ebeam}} = 3.92147 \times 10^{-9}$ m^2, $I_0 = 122.73$ A, $\zeta = 1.1$, $\sigma_e = 0.0005$, $\lambda_1 = 4.17189$ nm, $\lambda_3 = 1.39063$ nm.

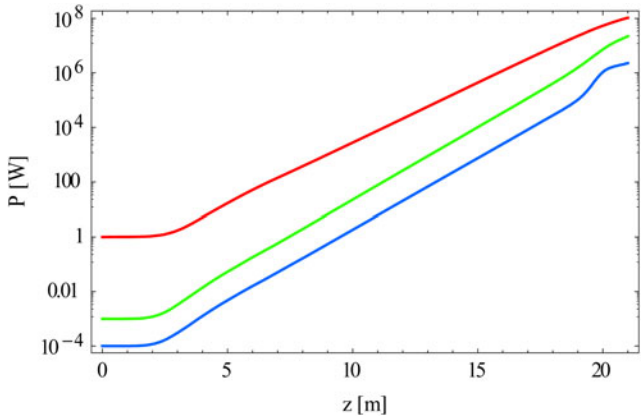


Fig. 5. SASE FEL harmonic power evolution with the two-frequency undulator: $n = 1$ – red line, $n = 3$ – green line, $n = 5$ – blue line. The parameters are as follows: $k = 2.133$, $h = 3$, $d = -0.5$, $\lambda_u = 0.028$ m, $\gamma = 1506.85$, $P_E = 103.95$ GW, $J = 9.96573 \times 10^9$ A/m^2, $\Sigma_{\text{ebeam}} = 4.31362 \times 10^{-9}$ m^2, $\lambda_1 = 20.5816$ nm, $\lambda_3 = 6.86053$ nm, $\lambda_5 = 4.11632$ nm, $\sigma_\varepsilon = 0.0001$.

https://doi.org/10.1017/S0263034617000180 Published online by Cambridge University Press

schemes are used. We will demonstrate it in forthcoming publications.

Now let us consider the simulation of the FEL with the same as before two-frequency undulator and electron beam with very low spread $\sigma_\varepsilon = 0.0001$, which is still possible for the energy $E = 0.75$ GeV. The evolution of the harmonic power in the framework of the phenomenological FEL model is presented in Figure 5.

Taken such high-quality beam we obtain even shorter gain length $L_{\text{gain}} = 0.997478$ m and saturation length $L_s = 22.6088$ m. Figure 5 evidences that the harmonic power in the two-frequency undulator becomes significant, ~1 and ~10 MW for the fifth and the third harmonics, respectively. The power growth is about 6–7 orders with respect to the low seed power at the fundamental frequency, the latter being n times lower than the harmonic frequency. The evolution of the power of high harmonics develops practically parallel to the fundamental harmonic power growth and it occurs in linear regime. Such behavior is due to the fact that in two-frequency undulator the Bessel functions for high harmonics have values comparable with the Bessel function values for the fundamental harmonic (see Zhukovsky, 2015*a*, *b*, *c*, 2016*a*, *b*), provided the losses are low as assumed. The domain of nonlinear generation, which is distinguished for the rapid growth of high harmonics at the end of the FEL undulator, reduces in the case of the two-frequency undulator. The power of the fundamental harmonic is practically the same as in common undulator: $P_{1,\text{F}} \sim 10^8$ W, but for the 5th harmonic we obtain up to 10^6 times growth over the seed of the fundamental harmonic, which is almost 100 times more than in a common undulator. In the considered case, we have this amplification at the Roentgen wavelength $\lambda_5 \approx 4$ nm at just ~20 m in SASE FEL, which is times shorter than the FEL length ~70 m required to saturate the fundamental harmonic with such frequency.

The evolution of the bunching coefficients b_n^2 in the above considered undulator is simulated in Figure 6, the parameters remain the same as in Figure 5.

As well as for the power evolution in Figure 5, in the case of the highly monoenergetic beam with $\sigma_\varepsilon = 0.0001$ the bunching for high harmonics follows the evolution of the bunching for the fundamental harmonic in linear regime as seen in Figure 6 and the lasing effect for high harmonics in big part occurs due to the bunching on the harmonic wavelengths $\lambda_n = \lambda_0/n$ and not only due to the bunching on the fundamental wavelength λ_0 as it happens for common undulator. In the case of a common planar undulator, the bunching coefficients for high harmonics grow slowly until nonlinear regime kicks in after 15 m. Proper figure for a common planar undulator is omitted for the sake of conciseness.

The evolution of the energy spread in FEL is essential, for example, for constructing cascade undulators. In Figure 7, we present the evolution of the energy spread along the two-frequency undulator in SASE FEL in the case of the high-quality electron beam (same beam as in Figs 5 and 6) with low energy spread $\sigma_\varepsilon = 0.0001$. As follows from Figure 7 our FEL induces the energy spread, such that at the critical length $z = 18.2626$ m the total energy spread reaches the maximum value, determined by the requirement $\sigma_\varepsilon \le \rho/2$ for the fifth harmonic; in our case it is $\sigma_\varepsilon = 0.000484926$. Indeed, for the Pierce parameter even with account for the diffraction correction we have $\rho_n^{\text{D}} = \{0.00129573, 0.00112146, 0.000973682\}$ for the harmonics with $n = 1, 3, 5$. The corresponding values of the bunching read as follows:

$$\begin{aligned} z &= 18.2626\,\text{m}, \\ b^2_{n=1,3,5} &= \{0.0678662,\ 0.0144286,\ 0.00116554\}. \end{aligned} \tag{22}$$

At the same time the squared value of the bunching for the third and for the fifth harmonics, induced by the fundamental harmonic, read: $|b_n|^2 \cong c_n |b_1|^{2n}$, where $c_1 = 1$, $c_3 = 6$, $c_5 = 60$; this yields for $b_1^2 = 0.0678662$ [see (22)] the following values:

$$\begin{aligned} b_1^2 &= 0.0678662, \\ b^2_{3,5\text{induced}} &= \{0.00187548, 0.0000863811\}. \end{aligned} \tag{23}$$

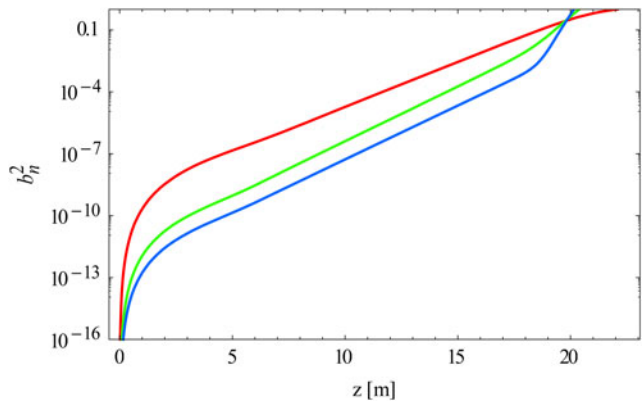


Fig. 6. Evolution of the bunching coefficients $b_n^2(z)$ for SASE FEL with two-frequency undulator: $n = 1$ – red line, $n = 3$ – green line, $n = 5$ – blue line. The values of the parameters are the same as given in Figure 5.

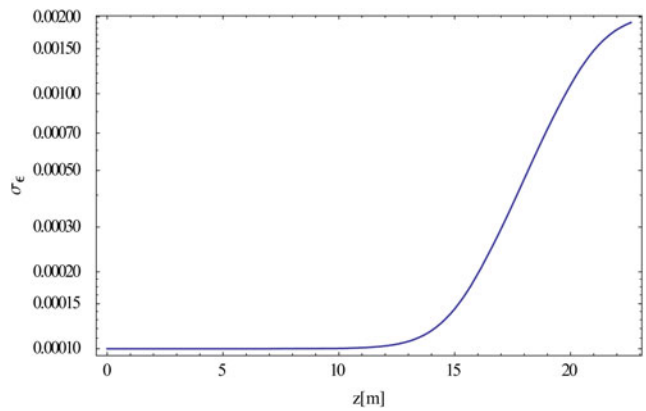


Fig. 7. Evolution of the energy spread in SASE FEL with two-frequency undulator.

https://doi.org/10.1017/S0263034617000180 Published online by Cambridge University Press

Upon the comparison of (22) and (23) we conclude that the induced by the fundamental harmonic values (23) are almost one order less than those due to the independent growth (22) and in the two-frequency undulator we have approximately one order of magnitude stronger bunching of high harmonics than in the common undulator; in the latter it is largely determined by power growth of the fundamental harmonic. This fact is important for building a cascade FEL, in which the last section is tuned on the harmonic of the preceding sections. Owing to this fact the two-frequency undulator appears particularly appealing solution in the cascade high-gain harmonic generation SASE FEL. Indeed, the last amplifer–radiator section, tuned at the third or at the fifth harmonic of the two-frequency undulator prebuncher section, gets already quite strong bunching [see (22)] at short length $z = 18.2$ m, in particular as compared with that in the case of a common planar undulator. Moreover, the amplifier-radiator gets the electron beam with low induced energy spread. Thus the beam, prebunched in the two-frequency undulator at the third or the fifth harmonic wavelength, can be efficiently used for further amplification of the proper harmonic in the amplifier section. The details will be addressed in a forthcoming publication.

6. CONCLUSIONS

We have considered the phenomenological model of SASE FEL, which describes the evolution of the FEL harmonic power and of the harmonic bunching coefficients along the FEL length. The model was verified and calibrated with the SASE FEL experiment. The input values for the simulation were taken from the experimental data. The simulated results agree well with the experimental values; their match is superior to many complicated numerical simulations. Thus, despite the complexity of underlying physical processes, regarding the interaction of the wave with the electrons with different energies, positions, and speeds, the phenomenological model catches the FEL physics and correctly accounts for the beam properties and losses, predicting true SASE FEL dynamics. The model calculations do not require powerful computational facilities or C++ programming, and it can be realized, for example, in simple and short Mathematica code, executed instantly.

The simulations of the FEL dynamics in the framework of the calibrated and verified phenomenological model were performed in Mathematica program both: for the two-frequency and for common undulators. They demonstrated that FEL with a two-frequency undulator is capable of delivering 10–100 times higher power at high harmonics than a common planar undulator does. As regards the Roentgen radiation, we showed that with the low energy $E \approx 0.75$ GeV electron beam and moderate current $I_0 \approx 150$ A in the double frequency undulator with the main period $\lambda_u = 2.8$ cm, the undulator parameter $k = 2.133$ and with the secondary periodic field given by (3), where $h = 3$, $d = -0.5$, an intense radiation in the near Roentgen range at $\lambda_5 \approx 4$ nm can be generated with significant power 100 kW–1 MW, dependently on the electron energy spread. This result can be achieved already at 25–30 m with the seeding laser wavelength $\lambda_1 \approx 20$ nm of 1 W power.

Using high-quality electron beam with low-energy spread in the two-frequency undulator we get early and significant growth of the high-harmonic power; the latter develops in linear regime. Moreover, the FEL with two-frequency undulator produces ten times stronger bunching for high harmonics right from the beginning of the FEL, differently from a common undulator, where the bunching for high harmonics is weak and its significant growth occurs mainly at the end, close to the saturation point and in nonlinear regime; it is in big part induced by the fundamental harmonic growth. This result is of particular significance for cascade FEL design, for example, for HGHG FEL, where the last section amplifies to saturation the high harmonic of the previous section. With the two-frequency undulator in the prebuncher section, the consequent amplifier–radiator gets the electron beam, which is strongly bunched at the high-harmonic length and the FEL-induced energy spread remains acceptably low. For example, for $\lambda_5 \approx 4$ nm the cut point for the two-frequency undulator prebuncher can be chosen at just 18.2 m.

This result paves the way to a powerful Roentgen FEL, working with high-quality low-energy electron beam with $\gamma < 1500$, and producing 10–100 MW power at relatively short length ~25–30 m.

ACKNOWLEDGMENT

The authors are grateful to Professor A.V. Borisov and Dr A. Lobanov for fruitful conversations and useful advices.

REFERENCES

Alferov, D.F., Bashmakov, U.A. & Cherenkov, P.A. (1989). Radiation from relativistic electrons in a magnetic undulator. *Usp. Fis. Nauk* **32**, 200–227.

Alferov, D.F., Bashmakov, Yu.A. & Bessonov, E.G. (1973). Radiation of relativistic particles in an undulator. *Sov. Phys. – Tech. Phys*. **17**, 1540–1550.

Artcimovich, A.L. & Pomeranchuk, I.J. (1945). Radiation from fast electrons in a magnetic field. *J. Phys. USSR* **9**, 267–276.

Artyukov, I.A., Bessonov, E.G. & Gorbunkov, M.V. (2016). Thomson linac-based X-ray generator: A primer for theory and design. *Laser Part. Beams* **34**, 637–644.

Bartnik, A., Fedosejevs, R., Wachulak, P., Fiedorowicz, H., Serbanescu, C., Saiz, E.G., Riley, D., Toleikis, S. & Neely, D. (2013). Photo-ionized neon plasmas induced by radiation pulses of a laser-plasma EUV source and a free electron laser FLASH. *Laser Part Beams* **31**, 195–201.

Bessonov, E.G. (2007). Light sources based on relativistic electron and ion beams. *Proc. SPIE* **6634**, article ID 66340X. doi: 10.1117/12.741920.

Bessonov, E.G., Gorbunkov, M.V., Ishkhanov, B.S., Kostryukov, P.V., Maslova, Yu., Y.A., Shvedunov, V.I., Tunkin, V.G. & Vinogradov, A.V. (2008). Laser-electron generator for X-ray applications in science and technology. *Laser Part Beams* **26**, 489–495.

https://doi.org/10.1017/S0263034617000180 Published online by Cambridge University Press

Bordovitsyn, V.A. (Ed.) (1999). *Synchrotron Radiation Theory and its Development: In the Memory of I.M.Ternov. Series on Synchrotron Radiation Technique and Applications*, Vol. 5. Singapore: World Scientific Publishing.

Dattoli, G. (1993). *Lectures on the Free Electron Lasers Theory and related Topics*, Vol. 637. Singapore: World Scientific Publishing.

Dattoli, G., Giannessi, L., Ottaviani, P.L. & Ronsivalle, C. (2004). Semi-analytical model of self-amplified spontaneous-emission free-electron lasers, including diffraction and pulse-propagation effects. *J. Appl. Phys*. **95**, 3206–3210. doi: 10.1063/1.1645979.

Dattoli, G., Mezi, L., Ottaviani, P.L. & Pagnutti, S. (2006*b*). Theory of high gain free-electron lasers operating with segmented undulators. *J. Appl. Phys*. **99**, 044907.1–044907.6. doi: 10.1063/1.2171810.

Dattoli, G., Mikhailin, V.V., Ottaviani, P.L. & Zhukovsky, K. (2006*a*). Two-frequency undulator and harmonic generation by an ultrarelativistic electron. *J. Appl. Phys*. **100**, 084507.1–084507.12.

Dattoli, G., Mikhailin, V.V. & Zhukovsky, K. (2008). Undulator radiation in a periodic magnetic field with a constant component. *J. Appl. Phys*. **104**, 124507.1–124507.8.

Dattoli, G., Mikhailin, V.V. & Zhukovsky, K.V. (2009). Influence of a constant magnetic field on the radiation of a planar undulator. *Moscow Univ. Phys. Bull*. **64**, 507–512.

Dattoli, G., Mirian, N.S., DiPalma, E. & Petrillo, V. (2014). Two-colour free-electron laser with two orthogonal undulators. *Phys. Rev. ST – AB* **17**, article ID 050702.

Dattoli, G., Ottaviani, P.L. & Pagnutti, S. (2005*b*). Nonlinear harmonic generation in high-gain free-electron lasers. *J. Appl. Phys*. **97**, 113102–1113102.7. doi: 10.1063/1.1886890.

Dattoli, G., Ottaviani, P.L. & Pagnutti, S. (2007). *Booklet for FEL Design*. Frascati, Italy: ENEA Pubblicazioni.

Dattoli, G., Ottaviani, P.L. & Renieri, A. (2005*a*). Free electron laser high gain devices. *Laser Part. Beams* **23**, 303–307.

Emma, P., Akre, R., Arthur, J., Bionta, R., Bostedt, C., Bozek, J., Brachmann, A., Bucksbaum, P., Coffee, R., Decker, F.-J., Ding, Y., Dowell, D., Edstrom, S., Fisher, A., Frisch, J., Gilevich, S., Hastings, J., Hays, G., Hering, Ph., Huang, Z., Iverson, R., Loos, H., Messerschmidt, M., Miahnahri, A., Moeller, S., Nuhn, H.-D., Pile, G., Ratner, D., Rzepiela, J., Schultz, D., Smith, T., Stefan, P., Tompkins, H., Turner, J., Welch, J., White, W., Wu, J., Yocky, G. & Galayda, J. (2010). First lasing and operation of an ångstrom-wavelength free-electron laser. *Nat. Photonics* **4**, 641–647. doi: 10.1038/NPHOTON.2010.176.

Giannessi, L., Alesini, D., Antici, P., Bacci, A., Bellaveglia, M., Boni, R., Boscolo, M., Briquez, F., Castellano, M., Catani, L., Chiadroni, E., Cianchi, A., Ciocci, F., Clozza, A., Couprie, M.E., Cultrera, L., Dattoli, G., Del Franco, M., Dipace, A., Di Pirro, G., Doria, A., Drago, A., Fawley, W.M., Ferrario, M., Ficcadenti, L., Filippetto, D., Frassetto, F., Freund, H.P., Fusco, V., Gallerano, G., Gallo, A., Gatti, G., Ghigo, A., Giovenale, E., Marinelli, A., Labat, M., Marchetti, B., Marcus, G., Marrelli, C., Mattioli, M., Migliorati, M., Moreno, M., Mostacci, A., Orlandi, G., Pace, E., Palumbo, L., Petralia, A., Petrarca, M., Petrillo, V., Poletto, L., Quattromini, M., Rau, J.V., Reiche, S., Ronsivalle, C., Rosenzweig, J., Rossi, A.R., Rossi Albertini, V., Sabia, E., Serafini, L., Serluca, M., Spassovsky, I., Spataro, B., Surrenti, V., Vaccarezza, C., Vescovi, M. & Vicario, C. (2011). Self-amplified spontaneous emission for a single pass free-electron laser. *Phys. Rev. ST-AB* **14**, article ID 060712. doi: 10.1103/PhysRevSTAB.14.060712.

Ginzburg, V.L. (1947). On the radiation of microradiowaves and their absorbtion in the air. *Isvestia Akademii Nauk SSSR (Fizika)* **11**, 165–169.

Huang, H. & Tallents, G.J. (2009). The output of a laser amplifier with simultaneous amplified spontaneous emission and an injected seed. *Laser Part Beams* **27**, 393–398.

Kumar, S., Kang, H.-S. & Kim, D.-E. (2012). For the generation of an intense isolated pulse in hard X-ray region using X-ray free electron laser. *Laser Part Beams* **30**, 397–406.

Lee, R.W., Baldis, H.A. & Cauble, R.C. (2002). Plasma-based studies with intense X-ray and particle beam sources. *Laser Part Beams* **20**, 527–536.

McNeil, B.W.J. & Thompson, N.R. (2010). X-ray free-electron lasers. *Nat. Photonics* **4**, 814–821. doi: 10.1038/nphoton.2010.239.

Mikhailin, V.V., Zhukovsky, K.V. & Kudiukova, A.I. (2014). On the radiation of a planar undulator with constant magnetic field on its axis taken into account. *J. Surf. Invest.: X-ray, Synchrotron Neutron Tech*. **8**, 422–428.

Mirian, N.S., Dattoli, G., DiPalma, E. & Petrillo, V. (2014). Production and properties of two-color radiation generated by using a Free-Electron Laser with two orthogonal undulators. *Nucl. Instrum.* A **767**, 227–234.

Mishra, G., Gehlot, M. & Hussain, J.-K. (2009). Spectral properties of bi-harmonic undulator radiation. *Nucl. Instrum. A*. **603**, 495–503.

Motz, H., Thon, W. & Whitehurst, R.N.J. (1953). Experiments on radiation by fast electron beams. *Appl. Phys*. **24**, 826–832.

Quattromini, M., Artioli, M., Di Palma, E., Petralia, A. & Giannessi, L. (2012). Focusing properties of linear undulators. *Phys. Rev ST – AB* **15**, article ID 080704. doi: 10.1103/PhysRevSTAB.15.080704.

Ternov, I.M., Mikhailin, V.V. & Khalilov, V.R. (1985). *Synchrotron Radiation and its Applications*. (translated from the Russian by S.J. Amoretty). Chur, London, Paris, New York (NY): Harwood Academic Publishers.

Tripathi, S. & Mishra, G. (2011). Three frequency undulator radiation and free electron laser gain. *Rom. J. Phys*. **56**, 411–424.

Vagin, P. V., Englisch, U., Müller, T. & Tischer, M. (2011). Commissioning experience with insertion devices at PETRA III. *J. Surf. Invest.: X-ray, Synchrotron Neutron Tech*. **6**, 1055–1057.

Zastrau, U., Burian, T. & Chalupsky, J. (2012). XUV spectroscopic characterization of warm dense aluminum plasmas generated by the free-electron-laser FLASH. *Laser Part. Beams* **30**, 45–56.

Zhirong, H. & Kwang-Je, K. (2007). Review of x-ray free-electron laser theory. *Phys. Rev. ST – AB* **10**, article ID 034801. doi: 10.1103/PhysRevSTAB.10.034801.

Zhukovsky, K. (2012). Undulator radiation in multiple magnetic fields. In *Synchrotron: Design, Properties and Applications* (Chua, D.M. and Toh, H.F., Eds), pp. 39–92. New York (NY), USA: Nova Science Publishers, Inc.

Zhukovsky, K. (2014*b*). Analytical account for a planar undulator performance in a constant magnetic field. *J. Electromagn. Wave* **28**, 1869–1887.

https://doi.org/10.1017/S0263034617000180 Published online by Cambridge University Press

Zhukovsky, K. (2015*b*). Harmonic generation by ultrarelativistic electrons in a planar undulator and the emission-line broadening. *J. Electromagn. Wave* **29**, 132–142.

Zhukovsky, K. (2015*c*). High harmonic generation in the undulators for free electron lasers. *Opt. Commun*. **353**, 35–41.

Zhukovsky, K. (2016*a*). Emission and tuning of harmonics in a planar two-frequency undulator with account for broadening. *Laser Part. Beams* **34**, 447–456. doi: 10.1017/S0263034616000264.

Zhukovsky, K. (2016*b*). High harmonic generation in undulators for FEL. *Nucl. Instrum. B* **369**, 9–14. doi: 10.1016/j.nimb.2015.10.041.

Zhukovsky, K.V. (2014*a*). Inhomogeneous and homogeneous losses and magnetic field effect in planar undulator radiation. *Prog. Electromagn. Res. B* **59**, 245–256.

Zhukovsky, K.V. (2014*c*). A model for analytical description of magnetic field effects and losses in a planar undulator radiation. *J. Surf. Invest.: X-ray, Synchrotron Neutron Tech*. **8**, 1068–1081.

Zhukovsky, K.V. (2015*a*). Harmonic radiation in a double frequency undulator with account for broadening. *Moscow Univ. Phys. Bull*. **70**, 232–239.

Ziaja, B., Weckert, E. & Möller, T. (2007). Statistical model of radiation damage within an atomic cluster irradiated by photons from free-electron-laser. *Laser Part. Beams* **25**, 407–414.

https://doi.org/10.1017/S0263034617000180 Published online by Cambridge University Press